Scientia Horticulturae 321 (2023) 112259

Contents lists available at ScienceDirect

Scientia Horticulturae

journal homepage: www.elsevier.com/locate/scihorti

H3K9 methylation patterns during somatic embryogenic competence expression in tamarillo (*Solanum betaceum* Cav.)

Daniela Cordeiro [a,*], Yolanda Pérez-Pérez [b], Jorge Canhoto [a], Pilar S. Testillano [b,*], Sandra Correia [a,c,*]

[a] Department of Life Sciences, Centre for Functional Ecology, Laboratory Associate TERRA, University of Coimbra, Calçada Martim de Freitas, Coimbra 3000-456, Portugal
[b] Pollen Biotechnology of Crop Plants Group, Margarita Salas Center of Biological Research, CIB Margarita Salas-CSIC, Ramiro de Maeztu 9, Madrid 28040, Spain
[c] InnovPlantProtect CoLAb, Estrada de Gil Vaz, Elvas 7350-478, Portugal

ARTICLE INFO

Keywords:
Cell reprogramming
Epigenetics
H3K9me2
Immunofluorescence
Somatic embryogenesis
Totipotency
Woody species

ABSTRACT

The capacity to regenerate is intrinsic to plants and is the basis of natural asexual propagation and artificial cloning. Despite there are different ways of plant regeneration, they all require a change in cell fate and pluripotency reacquisition, in particular somatic embryogenesis. The mechanisms underlying somatic cell reprogramming for embryogenic competence acquisition, expression and maintenance remain not fully understood. These complex processes have been often associated with epigenetic markers, mainly DNA methylation, while little is known about the possible role of histone modifications. In the present study, the dynamics of global levels and distribution patterns of histone H3 methylation at lysine 9 (H3K9), a major repressive histone modification, were analyzed in somatic embryogenesis-induced cell lines with different embryogenic capacities and during somatic embryo initiation, in the woody species *Solanum betaceum*. Quantification of global H3K9 methylation showed similar levels in the three types of proliferating calli (embryogenic, long-term and non-embryogenic), kept in high sucrose and auxin-containing medium. Microscopic analyzes revealed heterogeneous cell organization and different cell types, particularly evident in embryogenic callus. The H3K9 dimethylation (H3K9me2) immunofluorescence signal was lower in nuclei of cells showing embryogenic-like and proliferating features, while labeling was higher in vacuolated, non-embryogenic cells with higher proliferation rates. By auxin removal, somatic embryo development was promoted in the embryogenic cell line. During the initiation of this process, increasing levels of global H3K9 methylation were found, together with increasing H3K9me2 immunofluorescence signals, especially in cells of the developing embryo. These results suggest that H3K9 methylation is involved in somatic embryo development, a developmental pathway in which this epigenetic mark could play a role in the gene transcription variation that is associated with embryogenic competence expression in *S. betaceum*. Altogether, these data provide new insights into the role of this epigenetic mark in somatic embryogenesis in trees, where scarce information is available.

1. Introduction

Somatic embryogenesis is a non-sexual embryogenesis process, in which somatic cells, following an appropriate stimulus, usually an auxin treatment, reprogram and develop into embryos able to regenerate a whole plant (Méndez-Hernández et al., 2019). This represents a powerful biotechnology tool for the clonal propagation of elite genotypes and improved plants. Moreover, somatic embryogenesis enables the study of plant developmental plasticity, including morphogenesis and embryo initiation and development (Fehér, 2019). However, despite the efforts to reveal the mechanisms that occur at a cellular level (Cordeiro et al., 2022; Testillano, 2019; Wójcik et al., 2020), plant cell reprogramming remains largely unclear. Thus, deeper knowledge is needed to overcome the recalcitrance of some species in expressing their cellular totipotency (Ochatt and Revilla, 2016).

Solanum betaceum Cav. is a solanaceous tree, commonly known as tree tomato or tamarillo, with increasing interest due to its edible and highly nutritious fruits (Wang and Zhu, 2020). This species is easily

* Corresponding authors.
E-mail addresses: danielacordeiro@outlook.pt (D. Cordeiro), testillano@cib.csic.es (P.S. Testillano), sandraimc@uc.pt (S. Correia).

https://doi.org/10.1016/j.scienta.2023.112259
Received 16 March 2023; Received in revised form 13 June 2023; Accepted 15 June 2023
Available online 20 June 2023
0304-4238/© 2023 The Authors. Published by Elsevier B.V. This is an open access article under the CC BY license (http://creativecommons.org/licenses/by/4.0/).

manipulated and regenerated *in vitro*, and several optimized protocols are currently available for its *in vitro* culture (Alves et al., 2017; Cordeiro et al., 2020, 2023; Correia et al., 2011, 2012a; Correia and Canhoto, 2018). In this species, somatic embryogenesis is efficiently achieved in several explants, mainly zygotic embryos or young leaves (Canhoto et al., 2005). Through a two-step process, initiated from the same explant, and under the same culture conditions, somatic cells dedifferentiate and form two types of calli – compact embryogenic callus (EC) and friable non-EC (NEC; Correia et al. 2019, 2012b). These calli, with distinct morphology and competencies, can be separated and kept in culture for several years. Effective plant regeneration occurs when EC is incubated in an auxin-free medium with lower sucrose levels, followed by transference to light (Correia and Canhoto, 2018). However, with subsequent subcultures in proliferation conditions, the embryogenic potential of EC decreases, until becoming unable to develop somatic embryos (Currais et al., 2013). Nevertheless, these cells can be maintained and proliferated (herein termed long-term callus, LTC). Thus, through somatic embryogenesis, genetically identical cell populations with different cell fates can be obtained in *S. betaceum*, which therefore constitutes a favorable system for the study of the molecular mechanisms underlying embryogenic competence acquisition, expression and maintenance in woody species.

Epigenetic regulation was proven to have a pivotal role in the maintenance of plant cell plasticity and in the capacity to continuously regenerate organs, or even whole individuals *in vitro* (Ibáñez et al., 2020; Us-Camas et al., 2014). Epigenetics is a stable and heritable change in gene expression without variation in the DNA sequence, which can be caused by DNA methylation, non-coding RNA-mediated regulation and/or histone modifications (Goldberg et al., 2007). These dynamic modifications affect chromatin structure and hence the accessibility to gene transcription. Thus, epigenetic mechanisms modulate the activity of the genes contributing to their activation or silencing. In plants, histone modifications in heterochromatin regions (densely packaged DNA), such as di/trimethylation of histone 3 at lysine 9 (H3K9me2/3) and H3K27me3, are associated with gene silencing and so are called repressive marks (Li et al., 2007). These modifications have been also associated with DNA hypermethylation (Vaillant and Paszkowski, 2007). In turn, euchromatin regions (less packaged DNA) are transcriptionally active and associated with active marks, such as H3 acetylation (Ac), H4Ac, H3K4me3 and H3K36me2/3 (Li et al., 2007).

In the last decade, several works highlighted the involvement of epigenetic marks in cell fate reprogramming, as occurs during the induction of somatic embryogenesis and somatic embryo development (Corredoira et al., 2017; El-Tantawy et al., 2014; Kumar and Van Staden, 2017; Lee and Seo, 2018; Nic-Can and De La Peña, 2014; Rodríguez-Sanz et al., 2014; Solís et al., 2015; Testillano, 2019). Nevertheless, the dynamics and role of histone methylation in induced embryogenesis are poorly understood. Only a few studies exist on such modifications, including in *Arabidopsis thaliana* (Parent et al., 2021), *Brassica napus* (Berenguer et al., 2017; Rodríguez-Sanz et al., 2014), *Coffea canephora* (Nic-Can et al., 2013), *Hevea brasiliensis* (Li et al., 2020), *Hordeum vulgare* (Berenguer et al., 2017) and *Quercus suber* (Pérez et al., 2015). In general, these reports consider this histone epigenetic mark as required for embryogenic development. Furthermore, epigenetic-related transcripts, including histone methyltransferases and POLYCOMB proteins, were found upregulated in EC when compared to NEC samples in *Vitis vinifera* (Dal Santo et al., 2022), and during microspore embryogenesis in *B. napus* (Rodríguez-Sanz et al., 2014b; Berenguer et al., 2017). Thus, the goal of this work was to analyze the H3K9 methylation levels and nuclear distribution patterns occurring in *S. betaceum* proliferating cell lines and during embryo development initiation. Evaluating these epigenetic dynamics would bring some clues about the molecular basis of embryogenic commitment and the loss of the embryogenic potential throughout subcultures.

2. Materials and methods

2.1. Plant material - calli proliferation and somatic embryo development

Solanum betaceum cell lines with distinct embryogenic competencies were used in this assay: embryogenic callus (EC, 2-year-old), non-EC (NEC, 10-year-old) and callus that lost its embryogenic potential through subcultures (long-term callus (LTC), 8-year-old). All these cell lines were obtained from leaf explants of *in vitro* proliferating shoots, following the methodology previously described (Correia and Canhoto, 2018). Calli proliferation (herein T0) was made in Murashige and Skoog medium (MS, Murashige and Skoog 1962, © Duchefa Biochemie, Haarlem, The Netherlands), supplemented with 20 μM Picloram (Sigma-Aldrich®, St. Louis, Missouri, USA) plus 9% (w/v) sucrose at pH 5.7, solidified with 0.25% (w/v) Phytagel™ (Sigma-Aldrich®) and incubated at 24 ± 1 °C under dark conditions. Calli was monthly subcultured. EC, LTC and NEC at T0 were sampled and analyzed. For somatic embryo development, EC was incubated in development medium - MS plus 4% (w/v) sucrose at pH 5.7 and solidified with 0.8% (w/v) agar, under dark conditions for four weeks. EC at one, two and four weeks of incubation (T1, T2 and T4) were sampled and analyzed. LTC was also incubated in development medium to be used as a control at T1.

2.2. Fixation and microscopic analysis

Samples of LTC at T0 and T1 and of EC at T0, T1, T2 and T4 were collected and fixed overnight at 4 °C with 4% paraformaldehyde in phosphate-buffered saline (PBS). Samples of NEC at T0 were placed in 4% paraformaldehyde plus 10% sucrose and subjected to vacuum infiltration before overnight incubation. After fixation, samples were transferred to 0.1% paraformaldehyde and incubated at 4 °C until further processing. Fixed samples were washed in PBS 1x three times for 5 min, dehydrated through an acetone series (30, 50, 70, 90, and 100%) and placed in infiltration solution (Technovit® 8100 basic solution plus hardener 1; Kulzer, Germany) for 48 h with agitation at 4 °C. Samples were then placed in plastic capsules and embedded in polymerisation solution (infiltration solution plus Technovit® 8100 hardener 2; Kulzer, Germany). Resin polymerization was carried out at 4 °C for 24 h The resin blocks were sectioned at 2 μm thickness using an ultramicrotome. For cellular structure analysis, sections were stained with toluidine blue, mounted with Eukitt® and observed under a bright-field microscope.

2.3. Global H3K9 methylation quantification

Samples of NEC at T0, LTC at T0 and T1 and EC at T0, T1, T2 and T4 were collected and frozen in liquid nitrogen. For each time point, at least two pools of biological replicates were used. Histone extraction was performed using the EpiQuik™ Global Histone H3-K9 Methylation Assay Kit (Epigentek, Farmingdale, NY, USA), following the manufacturer's instructions. Histone protein concentration was further measured using Bradford's method (Bradford, 1976) in three technical replicates. Then, histone protein concentration was adjusted to 300 ng/μl and H3K9 methylation detection was prepared in two technical replicates for each sample, following the manufacturers' instructions. Optical density (OD) was measured by absorbance at 450 nm on a microplate reader. The average of the blank OD readings was subtracted from the OD of the samples and the positive control. Results were presented as the mean H3K9 methylation quantification, calculated by dividing the OD of each replicate by the OD of the positive control, with ± SE. Significant differences were analyzed by one-way ANOVA ($p < 0.05$), followed by Tukey's multiple comparisons test.

2.4. Immunofluorescence assays

From the resin blocks described above, sections of 2 μm were cut and

placed on multi-well slides pre-treated with aminopropyltriethoxysilane (APTES). Immunofluorescence was performed, at room temperature, to localize H3K9me2. Sections were first hydrated with PBS 1x for 5 min and blocked with 5% (w/v) Bovine Serum Albumin (BSA) in PBS solution for 10 min. Then, incubation with anti-H3K9me2 rabbit polyclonal antibody (Diagenode, Liège, Belgium) diluted 1:50 in 1% BSA was performed for 1 h in a humid chamber. Negative control for each sample was prepared, by incubating with PBS 1x instead of the antibody. After five washing steps with PBS 1x, sections were incubated with Alexa Fluor 488-labelled anti-rabbit antibody (Molecular Probes, Oregon, USA) diluted 1:25 in 1% (w/v) BSA in PBS for 45 min in a humid chamber in the dark. Following other five washes with PBS 1x, nuclei were stained with 1 mg/ml 4.6-diamino-2-phenylindole (DAPI) with Triton X-100 for 10 min in the dark. Finally, sections were washed two times with sterile water, mounted in Mowiol® medium and stored at 4 °C, protected from light, for further analysis in a confocal microscope.

2.5. Confocal microscopy analysis

Confocal microscopy analysis was performed using a confocal laser scanning microscope (Leica TCS-SP5-AOBS, Vienna, Austria). Observations were performed with 40x objective with immersion oil. Lasers' excitation of 461 and 488 nm wavelengths were used for DAPI (nuclei, blue) and anti-H3K9me2 immunofluorescence (green) signals, respectively. Optical sections at 0.5 µm z-intervals were captured with imaging software (Leica software LCS version 2.5). Maximum projection images were collected using the same settings of excitation and capture in all samples, for a better and more accurate comparison of signal intensity.

3. Results

3.1. Typology and morphology of somatic embryogenesis-induced cell lines

Three different types of *S. betaceum* cell lines, obtained by somatic embryogenesis induction in leaf explants, were used in this assay. Although having the same genetic background, these cells have a distinct morphology and embryogenic competency (Fig. 1). In proliferation for 10 years, non-embryogenic callus (NEC) is a yellowish, smooth, friable, mucilaginous, and watery mass of undifferentiated cells with no

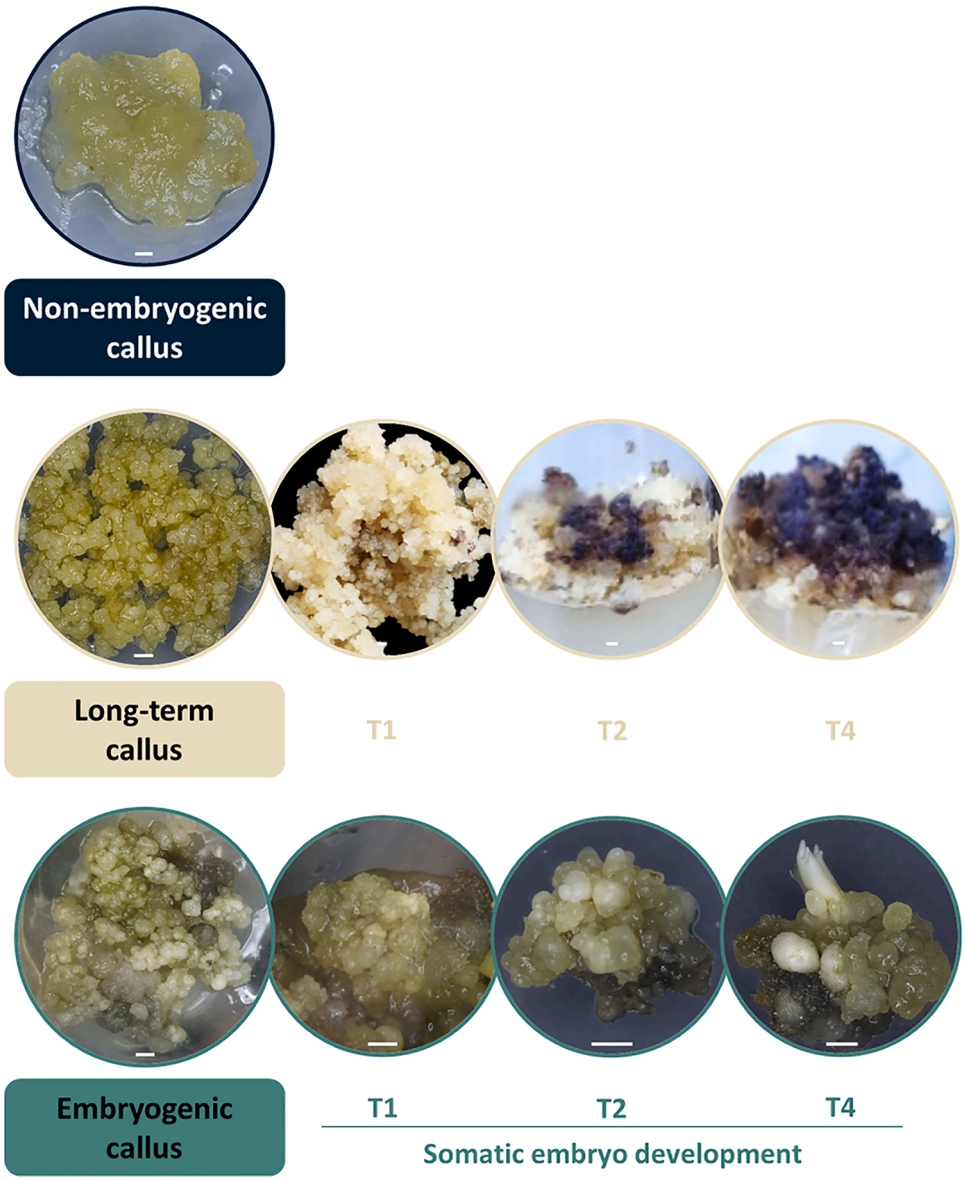

Fig. 1. *S. betaceum* somatic embryogenesis-induced cell lines (non-embryogenic, long-term and embryogenic callus) and somatic embryo development from the embryogenic callus line, at one (T1), two (T2) and four (T4) weeks in the auxin-free medium. Bars represent 1 mm.

embryogenic ability but with high proliferation capacity. In turn, embryogenic callus (EC), in slow proliferation for 2 years, is formed by whitish and compact globular clusters, able to develop somatic embryos when transferred to an auxin-free medium. With similar morphology, the 8-year-old long-term callus (LTC) is an older EC that, with subsequent subcultures, became unable to form embryos. Nevertheless, despite the loss of the embryogenic potential, NEC and LTC are easily distinguished by their different origins, and by their different morphological aspects, as NEC is a friable mass of dedifferentiated cells and LTC still resembles the whitish and more compact masses that compose EC lines. LTC cells continue to divide and proliferate, even at higher proliferation rates, as NEC.

To figure out whether H3K9 methylation is involved in the acquisition and loss of embryogenic competence throughout subcultures, those patterns were accessed in these cell lines. Moreover, H3K9 methylation was also analyzed during the embryogenic competence expression with somatic embryo development. Thus, the three calli were analyzed at the proliferation stage (T0), in which they are incubated in the presence of picloram (20 μM) and high (9%) sucrose levels. To induce embryo formation, EC was transferred to the development medium, in which the auxin was removed, and sucrose was reduced from 9% to 4% (w/v). During this process, three selected time points were studied, T1, T2 and T4, corresponding to one, two and four weeks after auxin removal (Fig. 1). Although no alteration was observed in the callus aspect, EC at one week of incubation (T1) in the development medium was analyzed to verify the effect of the auxin removal and sucrose reduction in the histone methylation patterns. As a control, LTC was also incubated in the development medium however, in the absence of auxin, no somatic embryos were formed, and strong tissue oxidation was observed after the first weeks of LTC in such conditions. Therefore, LTC was only analyzed at the end of one week (T1). At two weeks of incubation (T2), some white compact protuberances developing at the periphery of the EC clusters were observed and collected as putative somatic embryos developing structures. Although somatic embryo development was not synchronized, at four weeks (T4) white somatic embryos were formed, and further sampled and analyzed (Fig. 1).

3.2. Cellular structure analysis

To analyze the general structural organization at the cellular level of the different cell lines, semithin sections from resin-embedded samples were stained with toluidine blue and analyzed in a microscope under brightfield. Clear differences were found among NEC, LTC and EC (Fig. 2). NEC contained cells with heterogeneous sizes and shapes; in general, these cells were large with an elongated or rounded shape. In these cells, showing very large vacuoles and thin layers of cytoplasm, nuclei were located at the periphery (Fig. 2A). Contrary to NEC, LTC and EC showed a similar compact organization, with many cells cohesively positioned and forming round-shaped cell masses (Fig. 2B and C). However, LTC cells contained larger vacuoles and the nuclei were located at the cell periphery, as in NEC. Microscopic analysis revealed two different types of cells in EC: embryogenic cells distributed as groups or clusters (yellow arrow in Fig. 2C), surrounded by highly vacuolated cells, resembling NEC (black arrow in Fig. 2C and D). Embryogenic cells were small and isodiametric, like meristematic cells, showing large and round nuclei, occupying almost the entire cell (Fig. 2E). In addition, these cells displayed dense cytoplasm and appear to have small vacuoles and some granules.

Cell structural organization was also analyzed during somatic embryo development, in EC transferred to development medium (Fig. 3A–D). In general, cells became bigger and more vacuolated throughout this process (Fig. 3E–H). During the first week of incubation, embryo development started with the formation of small protrusions at the surface of the EC (Fig. 3A). Microscopic analyzes revealed that they were formed by a group of embryogenic cells localized at the periphery of the EC mass. They formed several layers of cells, characterized by small size, dense cytoplasm, and a big central nucleus (yellow arrow in Fig. 3E). Below these embryogenic cells, larger and highly vacuolated, non-embryogenic cells were observed (black arrow in Fig. 3E). With cell proliferation through time, the regions of embryo formation increased, and after around two weeks, they formed a larger group of cells that emerged over the surface of the EC (Fig. 3B and F). After 3–4 weeks, rounded protrusions (Fig. 3C and G) and early globular embryos (Fig. 3D and H), formed by cells with dense cytoplasm and large nuclei, appeared at the surface of the EC, which further developed and produced whole somatic embryos.

3.3. Global H3K9 methylation quantification

Using an ELISA-like assay for H3K9 methylation, global levels of H3K9 methylation were quantified at the proliferation stage (T0) of *S. betaceum* somatic embryogenesis-induced cell lines (NEC, LTC and EC), and during somatic embryo development, in EC (T1, T2 and T4). Proliferating NEC, LTC and EC showed moderate levels of global H3K9 methylation. NEC revealed slightly less H3K9 methylation compared to LTC and, at a bit higher level, compared to EC (Fig. 4). However, none of these differences were statistically significant. Then, LTC and EC were analyzed at one week in the development medium (T1). Although higher global H3K9 methylation levels were measured at this time-point compared with calli at T0, no statistically significant differences were found (Fig. 4). The highest changes in methylation levels occurred in EC during the following weeks, with somatic embryo development, which

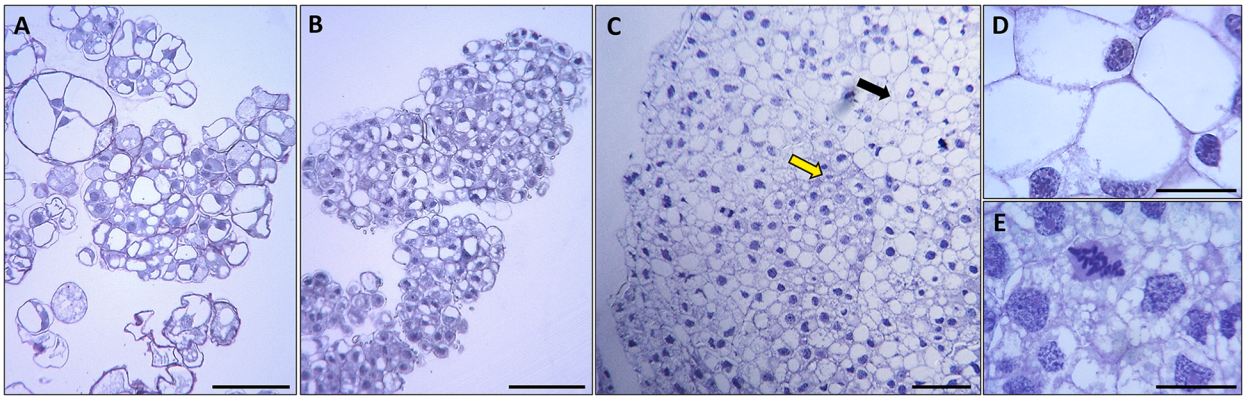

Fig. 2. Organization of the cell lines in the proliferation medium (T0). A - Non-embryogenic callus (NEC). B - Long-term callus (LTC). C - Embryogenic callus (EC). The black arrow shows non-embryogenic cells, and the yellow arrow shows embryogenic cells. D - Close-up of non-embryogenic cells from EC. E - Close-up of embryogenic cells from EC where several cells in mitosis can be seen. Images show micrographs of semithin sections stained with toluidine blue. Bars represent 100 μm in A-C and 25 μm in D-E.

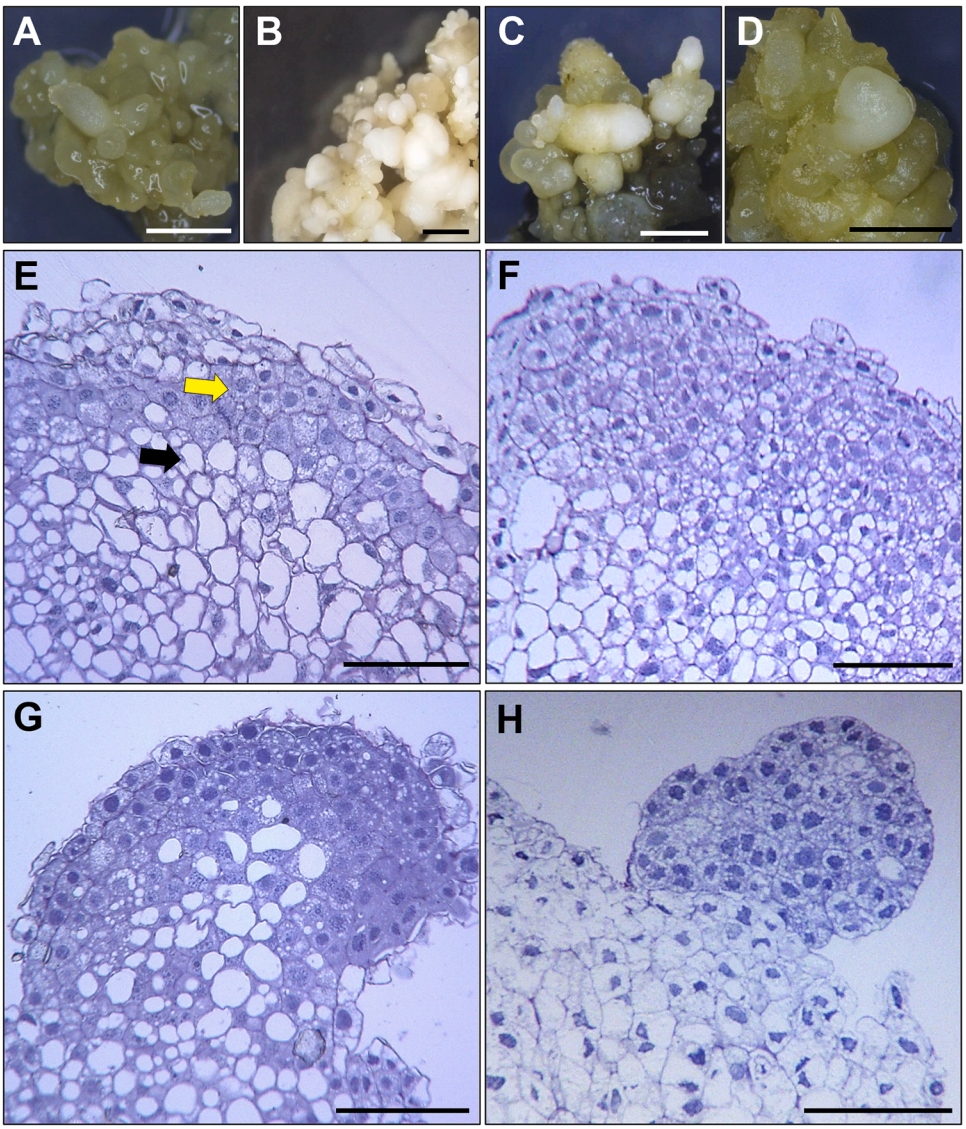

Fig. 3. Somatic embryo development from EC. Images show stereomicroscope observations and micrographs of semithin sections stained with toluidine blue at one (A, E), two (B, F) and four (C, D, G, H) weeks in the development medium. Developing embryos can be seen in figures C, D, G and H. The black arrow shows non-embryogenic cells, and the yellow arrow shows embryogenic cells. Bars represent 1 mm in A-D and 100 μm in E-H.

was accompanied by a gradual increase in global H3K9 methylation levels. Hence, at an advanced embryogenesis stage, with somatic embryo differentiation in EC at T4, the highest methylation levels were found (Fig. 4). This methylation degree was significantly different from the one measured for EC at T0 and to a higher extent from LTC and NEC at T0.

3.4. *H3K9me2 localization patterns*

Localization and distribution patterns of H3K9me2 were analyzed in proliferating cell lines with different embryogenic competencies, NEC, LTC and EC, and during the first stages of somatic embryo development. A specific antibody against H3K9me2 was used to perform the immunofluorescence assays. Confocal microscopy allowed signal visualization and maximum projections were used for comparison among samples. Images showed the high heterogeneity of the *S. betaceum* callus cell populations. A green fluorescence signal from H3K9me2 was observed over some of the blue-stained cell nuclei (DAPI) in all samples tested, and no signal background was observed in other cell compartments.

In the three types of cell lines, NEC (Fig. 5A), LTC (Fig. 5B) and EC (Fig. 5C), the H3K9me2 immunofluorescence signal was heterogeneously distributed among cells. Signal intensity was not similar in all cells, being intense in some nuclei while many other nuclei showed very low or null labeling (Fig. 5D–F), which resulted in a moderate level of global H3K9 methylation in the three cell lines, in accordance with the results of the ELISA assay. The number of positive nuclei and the intensity of the signal were variable in most samples, highlighting the cell heterogeneity present in these cell lines. In EC samples, labeling was often lower in rounded nuclei, corresponding to embryogenic cells. Controls avoiding the first antibody did not show labeling in any samples (Fig. 5G–I), supporting the specificity of the immunofluorescence assays.

During the first week of incubation in the development medium (after auxin removal), no significant changes were observed in LTC, neither in its cell organization nor in the labeling pattern of the H3K9me2, when compared with T0 (data not shown). In contrast, the transference of EC to the development medium resulted in the initiation of somatic embryo development. During the course of this process, in the subsequent weeks, the H3K9me2 signal progressively increased (Fig. 6). This result is in line with the quantification results (Fig. 4), which

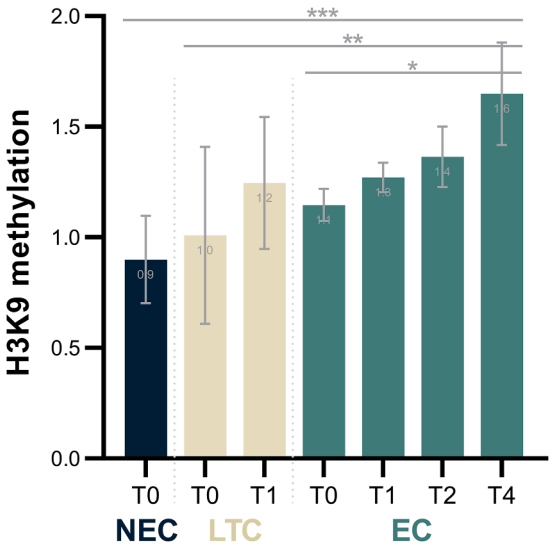

Fig. 4. Global H3K9 methylation quantification in non-embryogenic (NEC), long-term (LTC) and embryogenic callus (EC) at the proliferation stage (T0) and for one (T1), two (T2) and four (T4) weeks in the development medium. Results are presented as the mean H3K9 methylation quantification, calculated by dividing the OD of each sample by the OD of the positive control, ± SE. *, ** and *** indicate significant differences by one-way ANOVA and Tukey's test at $P \leq 0.05$, 0.005 and 0.0005, respectively.

showed a gradual increase in global H3K9 methylation levels, with significant higher levels in the advanced embryogenesis stage (EC at T4). The highest H3K9me2 immunofluorescence signal was observed on nuclei of cells that formed the incipient and large protrusions, and the developing embryos, emerging from the surface of EC (Fig. 6A–D, A'-D'). Immunofluorescence signal covered almost the entire area of the nuclei of developing embryos, while the rest of the cells showed less intense labeling, mainly in a few small spots over nuclei (Fig. 6A–D). This result indicates that the increase of H3K9me2 accompanies somatic embryo formation.

4. Discussion

Plant regeneration via somatic embryogenesis requires epigenetic reprogramming (Cordeiro et al., 2022; Fehér, 2015; Ibáñez et al., 2020; Nic-Can and De La Peña, 2014; Wójcikowska et al., 2020). Through this process, somatic cells dedifferentiate but not all are able to acquire embryogenic competence (Fehér, 2019). In this way, several genetic regulatory networks have been revealed as involved in the regulation of this capacity (revised in Wójcik et al. (2020)). These switches to new developmental programs require genome-wide changes, usually driven by epigenetic marks, including DNA and histone methylation, among other factors (Morończyk et al., 2022; Testillano et al., 2013; Wójcikowska et al., 2020). Also, several studies have reported the ubiquitous epigenetic changes associated with somatic embryogenesis initiation (Chen et al., 2020; De-la-Peña et al., 2015; Ibáñez et al., 2020). Nevertheless, epigenetic regulation of somatic embryogenesis, through H3K9 methylation, was not yet studied in long-term maintainable cultures.

Somatic embryogenesis in *S. betaceum* is a well-established two-step culture system, that not only provides a reliable and efficient means of producing large numbers of genetically identical plants (Correia et al., 2011) but can also be used for the conservation of selected germplasm (Graça et al., 2018), genetic transformation (Cordeiro et al., 2023) and fundamental research purposes (Correia et al., 2019). Nevertheless, several bottlenecks still impair a more efficient use of this system, including the loss of embryogenic competence during subcultures and the often-low embryo development rates from induced embryogenic cell lines (Correia et al., 2012a). Such bottlenecks are also commonly described for other species with two-step SE processes, such as alfalfa (Sangra et al., 2019), holm oak (Martínez et al., 2019) and Korean pine (Gao et al., 2021).

In this context, and since several reports relate cell reprogramming with epigenetic marks such as H3K9me, it is important to analyze those marks in systems with well-defined transitions between cellular stages, such as the one of *S. betaceum*. Therefore, to achieve a deeper knowledge of the mechanisms underlying embryogenic commitment, including acquisition, maintenance/loss and expression, the H3K9 methylation patterns were analyzed in *S. betaceum* cell lines with distinct embryogenic potential and during somatic embryo development. The analysis performed here reveals that, regardless of their embryogenic capacity, proliferating dedifferentiated cells from *S. betaceum* calli show moderate levels of global H3K9 methylation. Indeed, the establishment and maintenance of cell dedifferentiation require histone methylation activity (Grafi et al., 2007).

Microscopic analyzes indicate that embryogenic cell lines are heterogeneous and formed by different cell types. The H3K9me2 immunofluorescence assays revealed different signals between embryogenic and non-embryogenic cells in EC, as well as among distinct cells of NEC and LTC. Regardless of this cellular heterogeneity, the differences in the global H3K9 methylation levels among *S. betaceum* NEC, LTC and EC in proliferation were not statistically significant. These results suggest that H3K9 methylation might not have a significant role in the maintenance of the embryogenic potential during the proliferation stage of this species. Contrary, in cotton, enrichment in the H3K9me2 deposition was observed in EC when compared to NEC (Li et al., 2019), while in Norway spruce, higher H3K27me3 levels were reported in NEC when compared to EC (Nakamura et al., 2020).

During the initiation of *S. betaceum* somatic embryo development, a dynamic H3K9 methylation pattern was found. Both, the global H3K9 methylation levels and the H3K9me2 signal progressively increased, particularly in the cells of the developing embryo. Similarly, in *Coffea canephora*, an increase in the H3K9me2 levels was found during the whole somatic embryogenesis process, and mainly during somatic embryo development (Nic-Can et al., 2013). Moreover, these findings are in agreement with observations during the microspore embryogenesis of *Brassica napus* and *Hordeum vulgare,* in which H3K9 methylation increased during embryo development (Berenguer et al., 2017; Rodríguez-Sanz et al., 2014). However, active demethylation with lower H3K9me2 deposition was reported in cotton somatic embryos (Li et al., 2019). Nevertheless, increasing H3K9me2 is considered an epigenetic feature of cell differentiation (Ibáñez et al., 2020). In addition, H3K27me3 levels were also found to markedly increase upon embryo induction in Norway spruce (Nakamura et al., 2020). Altogether, these results corroborate that histone methylation is required for the embryogenic competence expression with embryo development. In the same way, this epigenetic mark was also found required for organogenesis, since an increase in H3K9 methylation was concomitant with needle maturation in *Pinus radiata* (Valledor et al., 2010).

As a repressive mark, H3K9 methylation is associated with chromatin condensation and gene silencing (Jackson et al., 2004). For instance, H3K9me2 was found to epigenetically modulate the transcription of *WUSCHEL RELATED HOMEOBOX4* (*WOX4*; Nic-Can et al., 2013). Authors claim that the repression of this transcription factor during somatic embryo maturation might be crucial for embryo elongation (Nic-Can et al., 2013). Similarly, for successful *in vitro* shoot regeneration in *Arabidopsis thaliana*, H3K9 methylation was found required to regulate the expression of the transcription factor *WUSCHEL* (Li et al., 2011). In addition, increases in histone methylation were associated with an increase in DNA methylation and also in the number of 24-nt siRNAs, particularly in EC and during embryo differentiation (Li et al., 2019; Solís et al., 2012). As the presence of auxins also affects the DNA methylation levels (De-la-Peña et al., 2015), to assure that the H3K9 methylation analyzed resulted from the embryo development *per*

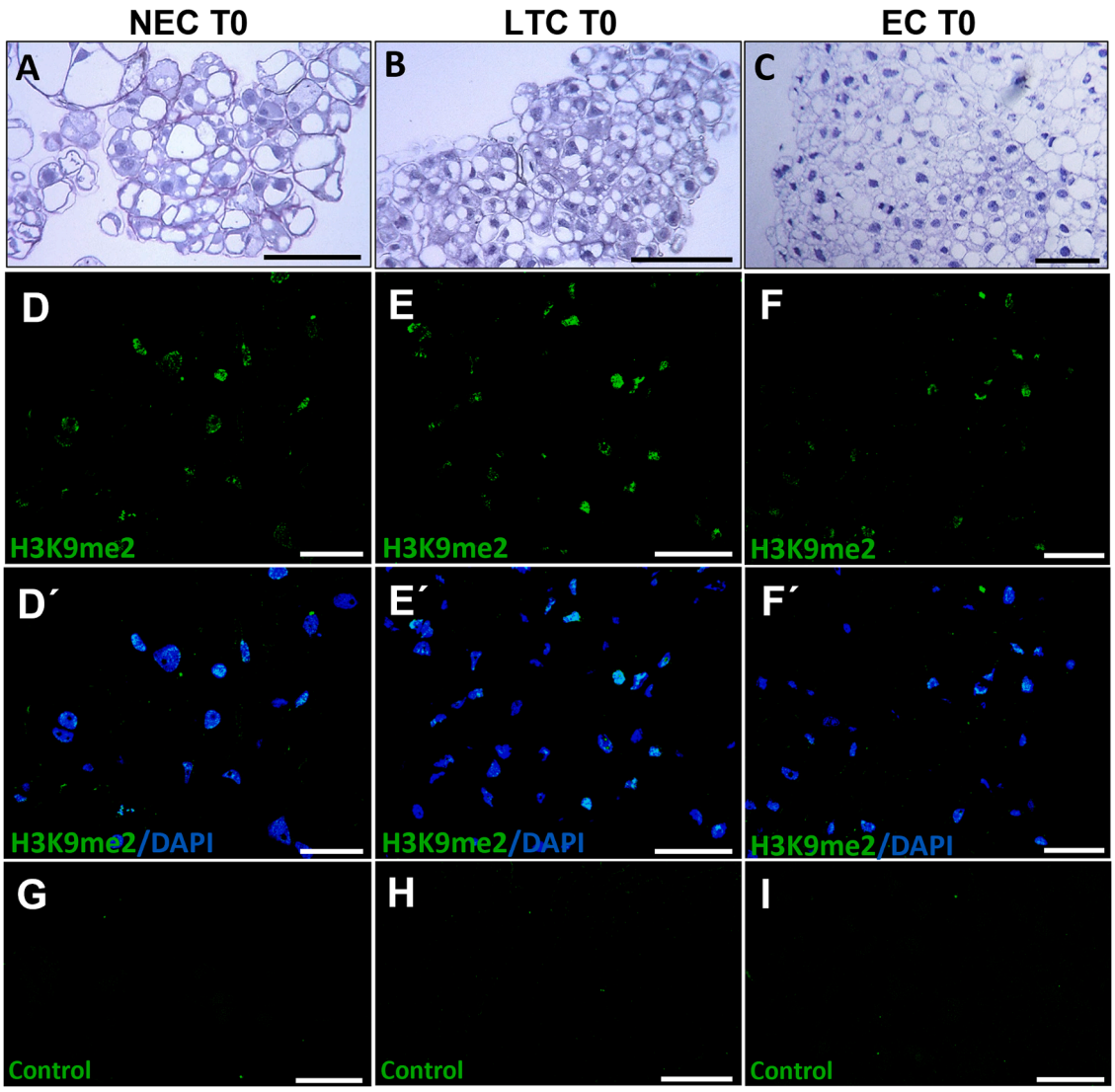

Fig. 5. H3K9me2 immunofluorescence in non-embryogenic callus (NEC), long-term callus (LTC) and embryogenic callus (EC) in proliferation medium (T0). A, B, C - Micrographs of semithin sections, stained with toluidine blue, showing the general structure of the three cell lines at T0. D, E, F – Confocal images of H3K9me2 immunofluorescence in NEC, LTC and EC, respectively. D', E', F' – Confocal merged images of H3K9me2 immunofluorescence signal (green) and DAPI staining of nuclei (blue) of the same regions as D-F. G, H, I - Controls avoiding the first antibody in NEC, LTC and EC, respectively. Bars represent 100 μm in A-C and 50 μm in D-F, D'-F' and G-I.

se and was not influenced by auxin removal, LTC was also incubated in the development medium. However, no changes were verified in the LTC methylation patterns, which proves that the increasing levels found in EC were in fact from cell embryo differentiation. Therefore, modulation of the H3K9 methylation process, with consequent genome-wide expression modification, could overcome embryogenesis recalcitrance and increase the efficiency of the somatic embryogenesis process in some angiosperms.

Another evident result of this work was the high cell heterogeneity among the different *S. betaceum* cell lines, which was already mentioned in previous works for EC and NEC (Correia et al., 2019, 2011). More notable was the cell heterogeneity revealed within each cell population, particularly EC which held embryogenic and non-embryogenic-like cells. While embryogenic cells showed a small and isodiametric shape and large nuclei, typical features of meristematic cells with high cell activity; non-embryogenic cells showed large vacuoles and peripherical positioned nuclei that are characteristics from undifferentiated tissues with low cellular activity. The presence of these two types of cells in the same tissue could affect the performance of *S. betaceum* EC in embryo development, resulting in low yield (Correia et al., 2012a). Moreover, the high cell heterogeneity resulted in a wide range of H3K9 methylation values measured in the various replicates. Also, a non-homogenous H3K9me2 immunofluorescence signal was observed among nuclei. Therefore, it is noteworthy that cell typology and histone methylation are related, which has already been reported in the literature for other species with two-step somatic embryogenesis processes (Nic-Can et al., 2013), and deserves further analysis.

5. Conclusion

Taken together, the results here presented indicated that plant cell reprogramming for the totipotency expression occurs with changes in the epigenetic mark H3K9 methylation. In this case, global H3K9 methylation, and hence gene transcription-repression, progressively increased during embryogenic competence expression, with the achievement of somatic embryo initiation and development. Although a certain level of global H3K9 methylation is present and possibly involved in the maintenance of the dedifferentiated and proliferative state of *S. betaceum* cell lines, independently of their embryogenic ability, as it increases after embryogenesis initiation, the role of this

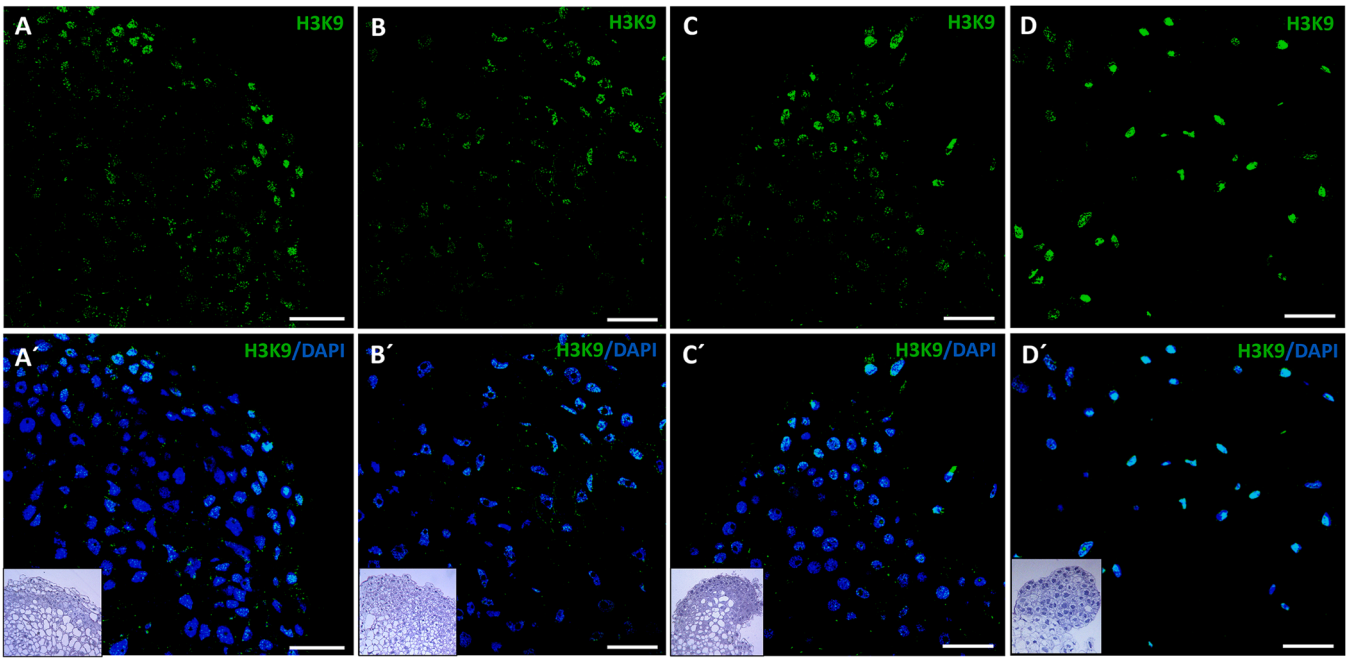

Fig. 6. H3K9me2 immunofluorescence during somatic embryo development from embryogenic callus, in subsequent weeks, from T0 to T4. A, B, C, D – Confocal images of H3K9me2 immunofluorescence signal (green). A', B', C', D' – Confocal merged images of H3K9me2 immunofluorescence signal (green) and DAPI staining of nuclei (blue) of the same regions as A-D. Inserts show analogous embryogenesis stages in semithin sections stained with toluidine blue. Bars represent 50 μm.

epigenetic mark would be associated with embryo differentiation. Therefore, this work represents a step further in the analysis of the molecular networks that regulate embryogenic competence in *S. betaceum* and other woody species with similar somatic embryogenesis systems.

Funding

This work was supported by Foundation for Science and Technology (Portugal), through PhD fellowship SFRH/BD/136925/2018 and COVID/BD/152914/2023 awarded to Daniela Cordeiro; Center for Functional Ecology—Science for People and the Planet (UIDB/04004/2020), financed by FCT/MCTES through national funds (PIDDAC); Cost Action 19125, through a Short-Term Scientific Mission awarded to Daniela Cordeiro; project PID2020-113018RB-I00, funded by Spanish MCIN/AEI/10.13039/501100011033 and projects TED2021-129633B-I00 and CPP2021-008750, funded by MCIN/AEI/10.13039/501100011033 and NextGenerationEU/ PRTR.

CRediT authorship contribution statement

Daniela Cordeiro: Conceptualization, Methodology, Validation, Investigation, Formal analysis, Writing – original draft, Visualization, Funding acquisition. **Yolanda Pérez-Pérez:** Conceptualization, Methodology, Validation, Investigation, Visualization. **Jorge Canhoto:** Conceptualization, Resources, Writing – review & editing, Funding acquisition. **Pilar S. Testillano:** Conceptualization, Methodology, Resources, Writing – review & editing, Visualization, Supervision, Funding acquisition. **Sandra Correia:** Conceptualization, Methodology, Resources, Writing – review & editing, Supervision, Funding acquisition.

Declaration of Competing Interest

The authors declare the following financial interests/personal relationships which may be considered as potential competing interests: Daniela Cordeiro reports financial support was provided by Foundation for Science and Technology. Daniela Cordeiro reports financial support was provided by Cost Action 19125. Pilar S. Testillano reports financial support was provided by Spain Ministry of Science and Innovation. Pilar S. Testillano reports financial support was provided by NextGeneration EU.

Data availability

No data was used for the research described in the article.

Acknowledgments

This manuscript is based upon work from COST Action COPYTREE CA21157, supported by COST (European Cooperation in Science and Technology).

References

Alves, A., Caeiro, A., Correia, S.I., Veríssimo, P., Canhoto, J., 2017. Establishment and biochemical characterization of tamarillo (*Solanum betaceum* Cav.) embryogenic cell suspension cultures. Vit. Cell. Dev. Biol. Plant 53, 606–618. https://doi.org/10.1007/s11627-017-9864-z.

Berenguer, E., Bárány, I., Solís, M.T., Pérez-Pérez, Y., Risueño, M.C., Testillano, P.S., 2017. Inhibition of histone H3K9 methylation by BIX-01294 promotes stress-induced microspore totipotency and enhances embryogenesis initiation. Front. Plant Sci. 8, 1161. https://doi.org/10.3389/fpls.2017.01161.

Bradford, M.M., 1976. A rapid and sensitive method for the quantitation of microgram quantities of protein utilizing the principle of protein-dye binding. Anal. Biochem. 72, 248–254. https://doi.org/10.1016/0003-2697(76)90527-3.

Canhoto, J.M., Lopes, M.L., Cruz, G.S., 2005. Protocol of somatic embryogenesis: tamarillo (*Cyphomandra betacea* (Cav.) Sendtn.). Protocol for Somatic Embryogenesis in Woody Plants. Springer, Dordrecht, pp. 379–389. https://doi.org/10.1007/1-4020-2985-3_30.

Chen, X., Xu, X., Shen, X., Li, H., Zhu, C., Chen, R., Munir, N., Zhang, Z., Chen, Y., Xuhan, X., Lin, Y., Lai, Z., 2020. Genome-wide investigation of DNA methylation dynamics reveals a critical role of DNA demethylation during the early somatic embryogenesis of *Dimocarpus longan* Lour. Tree Physiol. 40, 1807–1826. https://doi.org/10.1093/treephys/tpaa097.

Cordeiro, D., Alves, A., Ferraz, R., Casimiro, B., Canhoto, J., Correia, S., 2023. An efficient *Agrobacterium*-mediated genetic transformation method for *Solanum betaceum* Cav. embryogenic callus. Plants 12, 1202. https://doi.org/10.3390/plants12051202.

Cordeiro, D., Canhoto, J., Correia, S., 2022. Regulatory non-coding RNAs: emerging roles during plant cell reprogramming and *in vitro* regeneration. Front. Plant Sci. 13, 1049631 https://doi.org/10.3389/fpls.2022.1049631.
Cordeiro, D., Rito, M., Borges, F., Canhoto, J., Correia, S., 2020. Selection and validation of reference genes for qPCR analysis of miRNAs and their targets during somatic embryogenesis in tamarillo (*Solanum betaceum* Cav.). Plant Cell Tissue Organ. Cult. 143, 109–120. https://doi.org/10.1007/s11240-020-01901-7.
Corredoira, E., Cano, V., Bárány, I., Solís, M.T., Rodríguez, H., Vieitez, A.M., Risueño, M. C., Testillano, P.S., 2017. Initiation of leaf somatic embryogenesis involves high pectin esterification, auxin accumulation and DNA demethylation in *Quercus alba*. J. Plant Physiol. 213, 42–54. https://doi.org/10.1016/j.jplph.2017.02.012.
Correia, S., Alhinho, A.T., Casimiro, B., Miguel, C.M., Oliveira, M., Veríssimo, P., Canhoto, J., 2019. NEP-TC a rRNA methyltransferase involved on somatic embryogenesis of tamarillo (*Solanum betaceum* Cav.). Front. Plant Sci. 10, 438. https://doi.org/10.3389/fpls.2019.00438.
Correia, S., Canhoto, J.M., Jain, S.M., Gupta, P.K., 2018. Somatic embryogenesis of tamarillo (*Solanum betaceum* Cav.). Step Wise Protocols for Somatic Embryogenesis of Important Woody Plants. Springer, Cham, Switzerland, pp. 171–179. https://doi.org/10.1007/978-3-319-79087-9_14.
Correia, S., Cunha, A.E., Salgueiro, L., Canhoto, J.M., 2012a. Somatic embryogenesis in tamarillo (*Cyphomandra betacea*): approaches to increase efficiency of embryo formation and plant development. Plant Cell Tissue Organ. Cult. 109, 143–152. https://doi.org/10.1007/s11240-011-0082-9.
Correia, S., Lopes, M.L., Canhoto, J.M., 2011. Somatic embryogenesis induction system for cloning an adult *Cyphomandra betacea* (Cav.) Sendt. (tamarillo). Trees 25, 1009–1020. https://doi.org/10.1007/s00468-011-0575-5.
Correia, S., Vinhas, R., Manadas, B., Lourenço, A.S., Veríssimo, P., Canhoto, J.M., 2012b. Comparative proteomic analysis of auxin-induced embryogenic and nonembryogenic tissues of the solanaceous tree *Cyphomandra betacea* (tamarillo). J. Proteome Res. 11, 1666–1675. https://doi.org/10.1021/pr200856w.
Currais, L., Loureiro, J., Santos, C., Canhoto, J.M., 2013. Ploidy stability in embryogenic cultures and regenerated plantlets of tamarillo. Plant Cell Tissue Organ. Cult. 114, 149–159. https://doi.org/10.1007/s11240-013-0311-5.
Dal Santo, S., de Paoli, E., Pagliarani, C., Amato, A., Celii, M., Boccacci, P., Zenoni, S., Gambino, G., Perrone, I., 2022. Stress responses and epigenomic instability mark the loss of somatic embryogenesis competence in grapevine. Plant Physiol. 188, 490–508. https://doi.org/10.1093/plphys/kiab477.
De-la-Peña, C., Nic-Can, G.I., Galaz-Ávalos, R.M., Avilez-Montalvo, R., Loyola-Vargas, V. M., 2015. The role of chromatin modifications in somatic embryogenesis in plants. Front. Plant Sci. 6, 635. https://doi.org/10.3389/fpls.2015.00635.
El-Tantawy, A.A., Solís, M.T., Risueño, M.C., Testillano, P.S., 2014. Changes in DNA methylation levels and nuclear distribution patterns after microspore reprogramming to embryogenesis in barley. Cytogenet. Genome Res. 143, 200–208. https://doi.org/10.1159/000365232.
Fehér, A., 2019. Callus, dedifferentiation, totipotency, somatic embryogenesis: what these terms mean in the era of molecular plant biology? Front. Plant Sci. 10, 536. https://doi.org/10.3389/fpls.2019.00536.
Fehér, A., 2015. Somatic embryogenesis - stress-induced remodeling of plant cell fate. Biochim. Biophys. Acta Gene Regul. Mech. 1849, 385–402. https://doi.org/10.1016/j.bbagrm.2014.07.005.
Gao, F., Peng, C., Wang, H., Shen, H., Yang, L., 2021. Selection of culture conditions for callus induction and proliferation by somatic embryogenesis of *Pinus koraiensis*. J. For. Res. 32, 483–491. https://doi.org/10.1007/s11676-020-01147-1 (Harbin).
Goldberg, A.D., Allis, C.D., Bernstein, E., 2007. Epigenetics: a landscape takes shape. Cell 128, 635–638. https://doi.org/10.1016/j.cell.2007.02.006.
Graça, D., Correia, S., Ozudogru, E.A., Lambardi, M., Canhoto, J.M., Jain, S., Gupta, P., 2018. Cryopreservation of tamarillo (*Solanum betaceum* Cav.) embryogenic cultures. Step Wise Protocols for Somatic Embryogenesis of Important Woody Plants. Springer, Cham, pp. 95–101. https://doi.org/10.1007/978-3-319-79087-9_7.
Grafi, G., Ben-Meir, H., Avivi, Y., Moshe, M., Dahan, Y., Zemach, A., 2007. Histone methylation controls telomerase-independent telomere lengthening in cells undergoing dedifferentiation. Dev. Biol. 306, 838–846. https://doi.org/10.1016/j.ydbio.2007.03.023.
Ibáñez, S., Carneros, E., Testillano, P.S., Pérez-Pérez, J.M., 2020. Advances in plant regeneration: shake, rattle and roll. Plants 9, 897. https://doi.org/10.3390/plants9070897.
Jackson, J.P., Johnson, L., Jasencakova, Z., Zhang, X., PerezBurgos, L., Singh, P.B., Cheng, X., Schubert, I., Jenuwein, T., Jacobsen, S.E., 2004. Dimethylation of histone H3 lysine 9 is a critical mark for DNA methylation and gene silencing in *Arabidopsis thaliana*. Chromosoma 112, 308–315. https://doi.org/10.1007/s00412-004-0275-7.
Kumar, V., Van Staden, J., 2017. New insights into plant somatic embryogenesis: an epigenetic view. Acta Physiol. Plant 39, 1–17. https://doi.org/10.1007/s11738-017-2487-5.
Lee, K., Seo, P.J., 2018. Dynamic epigenetic changes during plant regeneration. Trends Plant Sci. 23, 235–247. https://doi.org/10.1016/j.tplants.2017.11.009.
Li, B., Carey, M., Workman, J.L., 2007. The role of chromatin during transcription. Cell 128, 707–719. https://doi.org/10.1016/j.cell.2007.01.015.
Li, H.L., Guo, D., Zhu, J.H., Wang, Y., Peng, S.Q., 2020. Identification of histone methylation modifiers and their expression patterns during somatic embryogenesis in *Hevea brasiliensis*. Genet. Mol. Biol. 43, 4. https://doi.org/10.1590/1678-4685-gmb-2018-0141.
Li, J., Wang, M., Li, Y., Zhang, Q., Lindsey, K., Daniell, H., Jin, S., Zhang, X., 2019. Multi-omics analyses reveal epigenomics basis for cotton somatic embryogenesis through successive regeneration acclimation process. Plant Biotechnol. J. 17, 435. https://doi.org/10.1111/pbi.12988.
Li, W., Liu, H., Cheng, Z.J., Su, Y.H., Han, H.N., Zhang, Y., Zhang, X.S., 2011. DNA methylation and histone modifications regulate *de novo* shoot regeneration in *Arabidopsis* by modulating *WUSCHEL* expression and auxin signaling. PLoS Genet. 7, e1002243 https://doi.org/10.1371/journal.pgen.1002243.
Martínez, M.T., San-José, M.D.C., Arrillaga, I., Cano, V., Morcillo, M., Cernadas, M.J., Corredoira, E., 2019. Holm oak somatic embryogenesis: current status and future perspectives. Front. Plant Sci. 10, 239. https://doi.org/10.3389/FPLS.2019.00239/BIBTEX.
Méndez-Hernández, H.A., Ledezma-Rodríguez, M., Avilez-Montalvo, R.N., Juárez-Gómez, Y.L., Skeete, A., Avilez-Montalvo, J., De-La-Peña, C., Loyola-Vargas, V.M., 2019. Signaling overview of plant somatic embryogenesis. Front. Plant Sci. 10, 77. https://doi.org/10.3389/fpls.2019.00077.
Morończyk, J., Braszewska, A., Wójcikowska, B., Chwiałkowska, K., Nowak, K., Wójcik, A.M., Kwaśniewski, M., Gaj, M.D., 2022. Insights into the histone acetylation-mediated regulation of the transcription factor genes that control the embryogenic transition in the somatic cells of Arabidopsis. Cells 11, 863. https://doi.org/10.3390/cells11050863.
Murashige, T., Skoog, F., 1962. A revised medium for rapid growth and bio assays with tobacco tissue cultures. Physiol. Plant 15, 473–497. https://doi.org/10.1111/j.1399-3054.1962.tb08052.x.
Nakamura, M., Batista, R.A., Köhler, C., Hennig, L., 2020. Polycomb repressive complex 2-mediated histone modification H3K27me3 is associated with embryogenic potential in Norway spruce. J. Exp. Bot. 71, 6366–6378. https://doi.org/10.1093/jxb/eraa365.
Nic-Can, G.I., De La Peña, C., Alvarez-Venegas, R., De-la-Peña, C., Casas-Mollano, J., 2014. Epigenetic advances on somatic embryogenesis of agronomical and important crops. Epigenetics in Plants of Agronomic Importance: Fundamentals and Applications. Springer, Cham, pp. 91–109. https://doi.org/10.1007/978-3-319-07971-4_6.
Nic-Can, G.I., López-Torres, A., Barredo-Pool, F., Wrobel, K., Loyola-Vargas, V.M., Rojas-Herrera, R., De-la-Peña, C., 2013. New insights into somatic embryogenesis: *LEAFY COTYLEDON1, BABY BOOM1* and *WUSCHEL-RELATED HOMEOBOX4* are epigenetically regulated in *Coffea canephora*. PLoS One 8, e72160. https://doi.org/10.1371/journal.pone.0072160.
Ochatt, S.J., Revilla, M.A., 2016. From stress to embryos: some of the problems for induction and maturation of somatic embryos. Methods Mol. Biol. 1359, 523–536. https://doi.org/10.1007/978-1-4939-3061-6_31.
Parent, J.S., Cahn, J., Herridge, R.P., Grimanelli, D., Martienssen, R.A., 2021. Small RNAs guide histone methylation in *Arabidopsis* embryos. Genes Dev. 35 https://doi.org/10.1101/gad.343871.120.
Pérez, M., Cañal, M.J., Toorop, P.E., 2015. Expression analysis of epigenetic and abscisic acid-related genes during maturation of *Quercus suber* somatic embryos. Plant Cell Tissue Organ. Cult. 121, 353–366. https://doi.org/10.1007/s11240-014-0706-y.
Rodríguez-Sanz, H., Moreno-Romero, J., Solís, M.T., Köhler, C., Risueño, M.C., Testillano, P.S., 2014. Changes in histone methylation and acetylation during microspore reprogramming to embryogenesis occur concomitantly with Bn HKMT and Bn HAT expression and are associated with cell totipotency, proliferation, and differentiation in *Brassica napus*. Cytogenet. Genome Res. 143, 209–218. https://doi.org/10.1159/000365261.
Sangra, A., Shahin, L., Dhir, S.K., 2019. Long-term maintainable somatic embryogenesis system in alfalfa (*Medicago sativa*) using leaf explants: embryogenic sustainability approach. Plants 8, 278. https://doi.org/10.3390/plants8080278.
Solís, M.T., El-Tantawy, A.A., Cano, V., Risueño, M.C., Testillano, P.S., 2015. 5-azacytidine promotes microspore embryogenesis initiation by decreasing global DNA methylation, but prevents subsequent embryo development in rapeseed and barley. Front Plant Sci 6, 472. https://doi.org/10.3389/fpls.2015.00472.
Solís, M.T., Rodríguez-Serrano, M., Meijón, M., Cañal, M.J., Cifuentes, A., Risueño, M.C., Testillano, P.S., 2012. DNA methylation dynamics and *MET1a-like* gene expression changes during stress-induced pollen reprogramming to embryogenesis. J. Exp. Bot. 63, 6431–6444. https://doi.org/10.1093/jxb/ers298.
Testillano, P.S., 2019. Microspore embryogenesis: targeting the determinant factors of stress-induced cell reprogramming for crop improvement. J. Exp. Bot. 70, 2965–2978. https://doi.org/10.1093/jxb/ery464.
Testillano, P.S., Solís, M.T., Risueño, M.C., 2013. The 5-methyl-deoxy-cytidine (5mdC) localization to reveal *in situ* the dynamics of DNA methylation chromatin pattern in a variety of plant organ and tissue cells during development. Physiol. Plant 149, 104–113. https://doi.org/10.1111/ppl.12015.
Us-Camas, R., Rivera-Solís, G., Duarte-Aké, F., De-la-Peña, C., 2014. *In vitro* culture: an epigenetic challenge for plants. Plant Cell Tissue Organ. Cult. 118, 187–201. https://doi.org/10.1007/s11240-014-0482-8.
Vaillant, I., Paszkowski, J., 2007. Role of histone and DNA methylation in gene regulation. Curr. Opin. Plant Biol. 10, 528–533. https://doi.org/10.1016/j.pbi.2007.06.008.
Valledor, L., Meijón, M., Hasbún, R., Jesús Cañal, M., Rodríguez, R., 2010. Variations in DNA methylation, acetylated histone H4, and methylated histone H3 during *Pinus radiata* needle maturation in relation to the loss of *in vitro* organogenic capability. J. Plant Physiol. 167, 351–357. https://doi.org/10.1016/j.jplph.2009.09.018.
Wang, S., Zhu, F., 2020. Tamarillo (*Solanum betaceum*): chemical composition, biological properties, and product innovation. Trends Food Sci. Technol. 95, 45–58. https://doi.org/10.1016/j.tifs.2019.11.004.
Wójcik, A.M., Wójcikowska, B., Gaj, M.D., 2020. Current perspectives on the auxin-mediated genetic network that controls the induction of somatic embryogenesis in plants. Int. J. Mol. Sci. 21, 1333. https://doi.org/10.3390/ijms21041333.
Wójcikowska, B., Wójcik, A.M., Gaj, M.D., 2020. Epigenetic regulation of auxin-induced somatic embryogenesis in plants. Int. J. Mol. Sci. 21, 2307. https://doi.org/10.3390/ijms21072307.